Experimental study and analysis of inner-stiffened cold-formed SHS steel stub columns

Experimental study and analysis of inner-stiffened cold-formed SHS steel stub columns

Aizhu Zhu[1]; Hongping Zhu[1]; Xiaowu Zhang[1]; and Yong Lu[2,*]

[1] School of Civil Engineering and Mechanics, Huazhong University of Science and Technology, Wuhan, China

[2] Institute for Infrastructure and Environment, School of Engineering, The University of Edinburgh, The King's Buildings, Edinburgh EH9 3JL, U.K.

* Corresponding author, Email: yong.lu@ed.ac.uk

Abstract: A series of axial compression tests was conducted to investigate the compressive behaviour of cold-formed steel stub columns with relatively thick walls (6mm and 10mm, respectively). Four different inner-stiffener arrangements were considered. Tensile coupons were cut from different parts of the square hollow section (SHS) sections to obtain a full picture of the enhanced material properties due to the cold-forming process. A finite element model was also developed and employed to provide a numerical perspective of the behaviour of the SHS columns. The applicability of two code-specified methods for the calculation of the strength of thin-walled cold-formed SHS columns for the present thick-walled cases is examined. The comparison shows that the AISI (and similarly AS/NZS) method tends to overestimate the sectional strength for the unstiffened and partially stiffened 6-mm thick columns, but predicts generally well (with slight underestimate) in the cases of well-stiffened 6-mm columns and all the 10-mm thick columns. The GB method, on the other hand, appears to predict well for all cases where the stiffening effect was less significant, but underestimates the sectional strength in the well-stiffened cases.

Keywords: Cold-formed steel column; Inner stiffener; Axial compression test; Sectional capacity; Failure modes; FE analysis

1. Introduction

Thin-walled cold-formed structural steel sections with wall thickness ranging from 0.4 to 6mm are commonly used in construction due to their advantages of superior strength-to-self-weight ratio, ease of construction, and cost-effectiveness. Traditional thin-walled sections with a variety of open- and closed-section configurations have been studied extensively [1-8].

Cold-formed sections are manufactured at ambient temperature and hence undergo plastic deformations causing strain hardening of the material. Due to the varying level of plastic deformation within the cold-formed sections, the hardening effect is not uniform and the corner regions are usually the most affected areas. For thin-walled members, the effects of cold forming process on the strength enhancement of the cold-formed corners, the planar plates and the whole sections have been discussed in most of the above mentioned studies. Methods for taking into account the corner strength enhancements in the cross-section design for thin-walled members, using an effective average yield strength, have been incorporated into design codes such as AISI [9], AS/NZS standard [10], and Chinese GB code [11].

For tubular columns, buckling of the column walls is a typical problem, and in thin-walled cold-formed sections this is dealt with by adding inner stiffeners to provide continuous support to the thin walls so as to enhance the buckling stress. The effects of stiffeners on cold-formed channel and angle sections have thus also been a subject of extensive research [1,4,12].

With the development of cold forming technology, nowadays carbon steel plates of up to 25mm in thickness can be fabricated successfully into structural sections [13,14] . With thicker walls, larger overall sectional dimensions can be accommodated in cold-formed members, and this certainly helps broaden the application potential of such technologies. For example, large square and rectangular hollow sections (SHS and RHS) of 500×500×16mm

and 400×600×16mm have been fabricated and investigated [15]. In line with this trend, experimental and numerical research on cold-formed steel columns with wall thickness ranging from 6mm to 16mm has become a new theme of research in recent years.

Guo et al. [13] investigated the effect of the cold-forming process on the strengths of mild steel coupons (Grade Q235 carbon steel), taken from tubular columns with thicknesses of 8mm, 10mm, and 12mm, respectively. It was found that the strength in the planar coupons on average had a marginal increase of 4% as compared to unformed steel, whereas in the most-affected corner regions the strength had an average increase of as much as 44% as compared to the unformed coupons. Hu et al. [16] conducted experimental investigations on both the material properties and sectional strengths of the cold-formed steel SHS and RHS tubes (without any stiffeners) with plate thickness of 9.2mm. The yield strength of the cold-formed planar and corner coupons exhibited an enhancement of 10% and 47%, respectively, while the mean sectional strength achieved an enhancement of 20% and 13% when compared with the predicted strengths using AS/NZS [10] and GB codes [11], respectively. In the study conducted by Afshan et al.[7] and Rossi et al. [17], SHS and RHS sections (without stiffeners) of cold-formed carbon steel with wall thickness varying from 5mm to 6mm, the yield strength of the planar and corner coupons respectively exhibited an enhancement of about 9% and 26% comparing to the strength stated in the mill certificates. Tong et al. [18] conducted a test study on the residual stresses of cold-formed carbon steel with 10-mm and 16-mm thick walls, and proposed residual stress distribution patterns of the thick-walled SHS without stiffeners.

Despite growing attention and increased research, experimental data concerning cold-formed sections with thick walls is still quite limited. The suitability of extending the calculation methods in relevant design codes, which have originally been developed for cold-formed thin-walled sections, to thick-walled sections still require more experimental

evidences. Furthermore, the effectiveness of using longitudinal inner stiffeners to maximize the buckling resistance of the SHS and RHS steel sections in the case of thicker walls is yet to be investigated.

This paper presents an experimental study with associated finite element and code-oriented calculations of the cold-formed SHS carbon steel columns with 6-mm and 10-mm thick walls and involving different arrangements of longitudinal inner stiffeners. Both material and sectional investigations were conducted. In the material investigation, coupon specimens for planar plates, corners, welded plates and stiffeners were extracted from the columns and tested under axial tension to obtain the enhanced strength profile in the cold-formed sections. The section investigation was carried out via compression tests of the stub column specimens. The effects of different stiffener arrangements in terms of the number and width of the stiffeners on the rigidity, ductility, failure modes and the overall sectional strength are investigated. Two codified methods for the calculation of the strength of cold-formed thin-walled sections, namely the AISI [9] and GB [11] methods, are examined and discussed by comparing the predictions with the corresponding experimental results.

2. Experimental programme

2.1 Overview of the column test specimens

Totally 10 cold-formed steel stub columns, including 2 unstiffened and 8 longitudinally inner-stiffened SHS columns were tested under axial compression. Fig. 1 shows the unstiffened section and four stiffened sections with different number or width of the inner stiffeners. All tubular sections were formed by a cold-forming process, in which steel sheet was roll-formed into C-sections. For sections involving stiffeners, longitudinal stiffeners were inserted and welded at this stage using filet welds. Two C-sections (with or without stiffeners) were then put together and butt welded into the final tubular form according to prescribed configuration (Fig. 1).

The 10 SHS stub columns were arranged into two groups according to the two tubular thicknesses of 6mm and 10mm, respectively. The columns are designated according to the section configuration and wall thickness, for example “SHS-a-6”, where “SHS-a” indicates section “a” (or “b” to “e”, as shown in Fig. 1), and the number “6” indicates the thickness of the SHS tubes; “6” = 6mm, or “10” = 10mm. The thickness of the inner stiffeners was 6mm for all SHS-*-6 columns and 8mm for all SHS-*-10 columns. The width of the stiffeners was uniformly 40mm, except for section “d” where the width of stiffeners was 60mm.

All column specimens had the same design cross-sectional size of 200×200mm (Fig.1), and the same column length of 600mm. A steel end plate was welded at the top and bottom end, respectively. The overall size of the end-plates was 240×240mm, and the thickness was 10mm for the SHS-*-6 columns and 16mm for the SHS-*-10 columns.

The SHS-*-6 tubes were made from steel with nominal yield strength of 345MPa, while the SHS-*-10 tubes were made from steel with yield strength of 235MPa. The stiffeners of both 6mm and 8mm thickness are all of 345 MPa grade. All the fabrication process was finished in a roll forming steel plant.

2.2 Test of tensile coupons

Material test coupons were extracted from three representative regions of the cold-formed SHS columns, namely planar, corner, and weld regions. Coupons were also prepared for the stiffners. The planar, weld and stiffener coupons were cut in a plate shape of width 40mm and length about 300mm. The corner coupons were cut around the highly cold-worked corner region in an angle of 90° and length of 300-360mm. All the plate and corner coupons were processed into short standard tensile specimens according to established procedures [19]. The axial tension tests were conducted using a Universal Testing Machine.

Totally 24 steel tensile coupons in 8 groups were prepared, with each group consisting of 3 identical samples, as listed in Table 1. The specimens in Table 1 are labelled according to

the region where the coupon was taken, the wall thickness and the serial number in the same group. The regions are identified by the first letter, namely “P” for planar, “W” for weld, “C” for corner, and “S” for (inner) stiffener. Thus, specimen P-6-1 is a “Planner” coupon with 6-mm thick wall and is the first (of three) specimen in the group.

The measured stress-strain curves of the tensile coupons with thickness of 6mm and 10mm are shown in Figs. 2 and 3, respectively. All the curves do not exhibit a yielding plateau as typical for mild steel, due apparently to the cold-forming or welding process. The curves from the planar and corner coupons show a marked stress strengthening (hardening) stage, which represents another significant result of the cold-forming process. The ductility of the corner coupons is markedly smaller than the planar coupons due to the much higher level of plastic deformation that occurred in the corner regions during the cold-forming process. The 10-mm thick coupons show better ductility than the 6-mm thick coupons, and this is deemed to be related to the different types of steel used, namely 235MPa for the 10-mm specimens and 345MPa for the 6-mm specimens.

For a comparison of the yield strength, the 0.2% tensile proof strength ($\sigma_{0.2}$) is adopted as the yield stress. The cross-sectional area (A_0) is calculated from the measured dimensions of the coupons. Table 1 summarizes the results of the proof yield strength and the ultimate strength (σ_u) from all individual samples, as well as the average values for each sample group. The percentage increase of the average yield strength of of the weld and corner coupons with respect to the planar coupons are also shown in Table 1 (in the column labelled by “Δ”). The final rupture positions of all the tension coupons occurred within the gauge lengths. Thus all the coupons were successfully tested. Typical failure modes of these coupons are shown in Fig. 4.

From Table 1, it is clear that the ultimate and yield ($\sigma_{0.2}$) stresses of both the welded and corner coupons are much higher than the corresponding stresses of the planar coupons. For

the coupons with thickness of 6mm, the average yield stress of the welded and corner coupons are 535.5MPa and 539.8MPa, which are respectively 22.3% and 23.3% higher than the average yield stress of the planar coupons (437.9MPa). For coupons with thickness of 10mm, the corresponding values are 505MPa and 433.6MPa, which are respectively 32.3% and 13.6% higher than the yield strength of planner coupons (381.7MPa). Based on previous experimental studies [13, 16] for the type of sections under consideration, the yield strength of the planar portion would be about 4%~9% higher than the original unformed steel. Thus the yield strength of the unformed steel could be deduced from the planar coupon strength as a basis for estimating the total enhancement of the sectional strength with respect to the unformed steel strength.

As for the cold formed stiffeners of both thicknesses of 6mm and 8mm, their original steel grade was 345 MPa which was the same as the 6-mm column walls. The measured yield strengths were similar to those of the 6-mm planar coupons.

2.3 Test of stub columns

The measured total cross-sectional areas of the SHS columns A (inclusive of the stiffeners) and the ratio of the area of the inner stiffeners A_s to the area A are summarized in Table 2. The stub columns were tested under axial compression using a compression testing machine with a capacity of 5000kN. The test columns were mounted on a rigid base and the compressive load was applied from the top. A typical test setup of the column specimens is shown in Fig. 5. Two displacement meters were used to measure the axial displacements of the top plate, and four longitudinal strain gauges were installed at the mid-height to measure the axial strain of the steel tubes. To ensure that the load was applied evenly across the cross sections, a thin layer of fine sands was carefully applied at the top and bottom of the specimens. Meanwhile, preliminary tests within the elastic range were conducted during which the position of the specimen was adjusted to ensure that the measured strains from the four strain gauges were

evenly distributed. The adjustment was considered as satisfactory when the difference between each individual strain and the average strain was no greater than 5%. Considering the estimated axial load capacities of all column specimens and the convenience of controlling the loading process, a load interval of 200kN was applied before the total load reached 50% of the estimated capacity of a test column. After that a load interval of 100kN was applied until the maximum load. At each loading step the load was maintained for about 3 minutes for stabilization of the response and data recording.

3. Test results of the column specimens

3.1 Rigidity, ductility, and failure modes

Figs. 6 and 7 show the average sectional stress vs. average strain curves of column specimens with 6-mm and 10-mm thick tubular wall, respectively. The stress σ was obtained by dividing the total test load by the total area A shown in Table 2. The average strain ε was calculated according to the measured strains of the four gauges attached at the mid-height of the columns. It is noted that in some curves the maximum loading point was missing, and this was due to either or both of the following reasons, (1) the strain gauges attached at the mid-height of the specimens failed before the axial load reached the maximum bearing capacity; (2) the specimen failed with buckling of the steel tubes when the peak load was reached, featuring a rapid decline in the load carrying capacity accompanied by large axial deformation. It was difficult to record the final strains in such cases. Nevertheless, the peak loads were correctly captured by the testing machine for all specimens. It is also noted that specimen SHS-b-10 had failure of two gauges, so the corresponding σ - ε curve was not obtained.

As can be seen from Figs. 6 and 7, all σ - ε curves exhibit good linear behaviour until about 50% of the maximum stress. The normalised rigidity, i.e. the slope of the σ - ε curve, at this stage is found to be close to the Young’s modulus of normal steel, and it varied in a range

from 190GPa to 210GPa. The slopes of the curves tend to exhibit more noticable differences as the load increases, and this is particularly true for specimens with 6-mm thick tubes; the slopes during the second half loading stage generally increase with the sectional area of the inner stiffeners. For specimens with 10-mm thick tubes, however, only specimen SHS-e-10, which had a heavily arranged inner stiffeners (see Fig. 1), experienced a marked increase in the second-stage slope as compared with other specimens of the same wall-thickness. These results indicate that the normalised rigidity of the specimens with 10-mm tubes was not affected by the inner stiffeners unless a considerable amount of stiffeners was used (in the case of SHS-e-10, 8 stiffeners).

Generally speaking, all the columns exhibited substantial compressive deformability before the axial load reached the maximum sectional compressive stress. Specimens with a higher area ratio of stiffeners tend to show increased deformability. On average, the measured maximum axial strain at the compressive load approaching the peak load reached about 6000με in SHS-*-6 stub columns and about 8000με in SHS-*-10 stub columns. The higher measured maximum strain in SHS-*-10 columns may be attributed to the fact that the 10-mm thick steel was made of milder steel of 235MPa as compared to the 6-mm steel of 345MPa, and moreover, the thicker tubes had smaller width-to-thickness ratios and thus buckling generally occurred later than the thinner tubes.

Figs. 8 and 9 show typical failure modes for specimens with 6-mm and 10-mm thick tubular walls, respectively. It is noted that the tubular walls buckled either outward or inward from the surface of the tubular section. However, as shown in Figs. 8(b) and 9(b), the buckling deformation of the stiffened walls was clearly less severe than that of the unstiffened walls. Furthermore, comparing specimens SHS-c-6 with SHS-e-6, both of which had a doubly symmetrical arrangement of stiffners, the failure mode changed markedly when the number of stiffners increased from one (SHS-c-6) to two (SHS-e-6) on each side of the section. While

several outward bucklings events were observed along the height in SHS-c-6, local buckling was essentially prevented in SHS-e-6 and only one dominant outward bukling occurred, as shown in Figs. 8(c) and (e). This observation suggests that for the sections with wall thickness of 6mm in a 200-mm section, it would require more than one stiffner on each side of the section if local buckling was to be prevented. From the current stub column tests of both 6-mm and 10-mm thick walls, it appears that using more stiffeners is more effective than increasing the width of the stiffeners in resisting local buckling.

3.2 Sectional capacity and strength

The sectional capacity here is measured by the ultimate (maximum) axial compressive force N_u, and the nominal strength f_u is calculated as $f_u = N_u/A$, where A is the total sectional area. The test results of $N_{u,exp}$ and $f_{u,exp}$ of the cold-formed SHS columns are summarized in Table 2. The results of $N_{u,exp}$ and $f_{u,exp}$ are also plotted versus sectional area ratio A_s/A in Figs. 10 and 11, respectively. The following observations can be made:

(1) $N_{u,exp}$ in both 6-mm and 10-mm thick SHS columns generally increases almost proportionally with the increase of the ratio A_s/A. The increasing rate (slope) for the 6-mm columns appeared to be larger than that of the 10-mm columns, as represented by the linear fitting coefficients of 4497 for the 6-mm columns comparing with 4356 for the 10-mm columns. This indicates that for the thinner 6-mm columns the stiffeners had more added effect in alleviating buckling, besides the gross increase of the sectional area, than for the 10-mm columns.

(2) By plotting the normalised strength $f_{u,exp}$, shown in Fig. 11(a) for the 6-mm columns and Fig. 11(b) for the 10-mm columns, the net enhancement effect of stiffeners on the ultimate strength of the SHS columns can be more conveniently observed. Comparing the two sets of results in Fig. 11, it is clear that there is marked buckling-resistance effect of using stiffeners in the 6-mm columns, whereas such effect tends to diminish when the wall

thickness increased to 10-mm for the 200mm cross-section SHS columns herein. Moreover, within the 6-mm group columns, the most significant increase of $f_{u,exp}$ (see Table 2 for $\Delta f_{u,exp}$) in the stiffened columns as compared the unstiffened column SHS-a-6 was 13.7%, which occurred in SHS-c-6 when four inner stiffeners of width 40mm were used. A marginal increase in specimens SHS-b-6 by 1.24% indicates that the stiffening effect of using just two inner stiffeners was not effective. On the other hand, the $f_{u,exp}$ values in specimens SHS-d-6 and SHS-e-6 were similar to SHS-c-6, and this suggests that using much wider or more inner stiffeners did not result in further enhancement in the ultiamet strength.

(3) With regard to the hardening effect of the cold-forming process on the overall SHS column strength, the unstiffened specimen SHS-a-10 may be used as a good benchmark as it did not involve any stiffeners and local bucking did not seem to affect the column strength significantly as discussed above. The measured strength $f_{u,exp}$ in this column is 418.6MPa, which is about 10% higher than the tensile strength of the 10-mm planar plates (381.7MPa, see Table 1). This is apparently attributable to the contribution of the enhanced corner and welded parts of the tubular sections from the cold-forming process. For the 6-mm thick reference specimen SHS-a-6, however, the measured strength $f_{u,exp}$ is 400.6MPa, which is about 10% lower than the yield strength of the 6-mm planar plates (437.9MPa). This can be explained by the fact that, despite the enhanced strength in the corner and welded parts, the the local buckling-stability factor still plays an important role in influencing the overall strength of the 6-mm thick columns due to a larger sectional width to thickness ratio of the unstiffened tubes.

(4) The above measured strength data and the associated observations concerning the relative effect of stiffeners and the cold-forming process on SHS columns can be used to verify the adequacy of adopting some existing methods to calculate the strength of SHS columns with thicker walls, and this will be discussed in Section 5.

4. Finite element (FE) analysis

To further understand the effects of the inner stiffeners on the performance of the SHS stub columns, a finite element (FE) analysis was conducted using ABAQUS. The nominal sectional dimensions shown in Fig.1 were used to build the FE models. The SHS tube was simulated by using shell element S4R. The two end-plates were simlpified as rigid plates and modeled using the discrete rigid body elements. The rigid end plates were attached to the SHS tube via shared nodes at the adjoining points. In order to model the boundary conditions in the test (see Fig.5), the bottom plate was assumed as being fully constrained while the top plate was loaded in the vertical direction.

A multi-linear stress versus strain curve for the cold-formed steel, introduced in [20], was used to simulate the material property of the SHS columns. The average test yield ($\sigma_{0.2}$) and ultimate (σ_u) stresses of the planar, welded, corner and stiffener coupons reported in Table 1 were used as yield and ultimate strengths to predict the steel stress-strain curve of the corresponding sectional parts. The reference Young's modulus E_s and Poisson's ratio of the steel tube are assumed to be 2.06×10^5MPa and 0.3, respectively.

In order to obtain an appropriate element mesh size, the FE model of Specimen SHS-a-6 was analyzed using three element sizes equal to 1/10, 1/20 and 1/40 of the sectional width, respectively. The calculated sectional capacity $N_{u,FEA}$ was 1723kN, 1715 kN and 1718 kN, respectively. The results can be considered as stable with all these mesh sizes. Thus the element size of 1/20 of the sectional width was finally used. The meshed model of SHS-*-6 specimens can be found in Fig. 12.

The eigenvalue buckling analysis of the SHS column specimens was conducted and initial geometric imperfection with the same distribution as the first-order eigenvector was introduced to the corresponding FE models to simulate the local buckling, where the maximum size of the imperfection was set to one-tenth of the corresponding wall thickness

[21]. The material strength is governed by the Mises Yield Criterion.

The FE predicted sectional stress-strain curves are shown in Figs. 6 and 7 for columns with 6-mm and 10-mm thick tubular wall, respectively, alongside the test results. The ratio of the predicted to the measured axial resistance capacity, $N_{u,FEA}/N_{u,exp}$, is also reported in Table 2. The variation curves of $N_{u,FEA}$ and sectional stress $f_{u,FEA}$ with the stiffner area ratio A_s/A are shown in Figs. 10 and 11, respectively.

As can be observed from Figs. 6 and 7, during the initial loading stage, the FE predicted σ - ε curves agree well with the test results. In terms of the ultimate capacity, the predicted and measured capacity ratio $N_{u,FEA}/N_{u,exp}$ ranges from 0.94 to 1.13, and mean value and standard deviation (SD) of all the ratios are 1.04 and 0.03, respectively. The variation of $N_{u.FEA}$ and stress $f_{u,FEA}$ with the ratio A_s/A in Figs. 10 and 11 also shows good agreement with the corresponding experimental curves. The FE model further complements the experimental curves in that a full process of the mechanical behaviour of the SHS column specimens, including the post peak branch, can be produced.

From the predicted σ - ε curves in Fig. 6, it can be found that Specimen SHS-b-6 exhibits a brittle failure mode with an abrupt unloading phase, and this behaviour agrees well with the experimental result. Other specimens of 6-mm thick walls with stiffeners showed improved ductility and sectional capacity.

For the SHS-*-10 specimens, the predicted σ - ε curves shown in Fig. 7 are in line with the test curves and the results tend to suggest that, a) the SHS-*-10 columns generaly possess better deformability than the SHS-*-6 columns, and this may be explained by both a milder steel and a smaller width-to-thickness ratio, and b) for SHS columns of this level of thickness, the effect of stiffeners would only become significant when the area ratio of the stiffeners (A_s/A) is large enough, such as in the cases of SHS-d-10 and SHS-e-10.

Fig.12 show typical failure modes of the specimens with 6-mm wall thickness obtained

from the FE analysis. Comparing to the experimental counterparts shown in Fig. 8, the FE results realistically captured the main local buckling occurrences (including outward and inward deformations). The FE predicted failure modes in columns of 10-mm wall thickness also show a favourable comparison with the corresponding experimental results.

5. Verification of relevant code methods for the calculation of SHS axial resistance capacities

As mentioned in Introduction, the exsiting calculation methods for cold-formed hollow steel sections in typical design codes have been derived largely from results of thin-walled members. In this section, selected code methods will be applied in the calculations of the test SHS columns and the results will be compared with the experimental data. Based on the comparisons, the adequacy of extending the use of these methods to SHS columns with thick walls is assessed and discussed.

5.1 AISI and AN/NZS method

According to Clause B2.1 of the North American Specification for Design of Cold-formed Steel Structural Members [9], as well as Clause 2.2.1 of the Standards Australia / Standards New Zealand for Cold-formed Steel Structures [10], it can be found that the effective width of the unstiffened SHS columns in both 6mm- and 10mm-thick wall groups is equal to the planar plate width. Therefore, the total sectional area in all cases can be used as the effective sectional area when predicting the sectional capacity of the columns. The design yield stress considering the effects of the cold-forming process can be calculated as Eq. (2) according to Clause A7.2 of the AISI specification:

$$f_{ya,AISI} = Cf_{yc} + Sf_{ys} + (1 - C - S) f_{yf} \tag{2}$$

where $f_{yc} = B_c f_{yv} / (r_i / t)^m$, and $B_c = 3.69 f_{uv} / f_{yv} - 0.819 (f_{uv} / f_{yv})^2 - 1.79$, $m = 0.192 f_{uv}/f_{yv} - 0.068$. In the calculation for the test columns, the stresses f_{uv} and f_{yv} are estimated from the

actual ultimate and yield stresses (average) σ_u and $\sigma_{0.2}$ of planar plates shown in Table 1, respectively. The measured ratio r_i/t shown in Table 2 was used. *C* and *S* are determined by the corresponding measured sectional areas. S equals to zero for specimens with unstiffened sections.

5.2 GB-2002 method

According to Appendix C in the Chinese Code GB50018[11], the average design yield stress considering the stress enhancement induced by the cold-forming process can be calculated by:

$$f_{ya,GB} = \left[1 + \frac{\eta(12\gamma - 10)t}{l} \sum_{i=1}^{n} \frac{\theta_i}{2\pi}\right] f_{yv} \qquad (3)$$

where the subscript "GB" is used to denote the GB code.

In this study, η = 1.0, γ = 1.58 and 1.48 for steel with nominal yield stress of 235MPa and 345MPa, respectively. As each column has four right-angle corners, the sum of the angle ratios $\theta_i/2\pi$ equals 1.0. The calculation of the centre-line length *l* is simplified as *A*/*t* for the specimens with unstiffened sections according to the recommendation in the GB code. For those specimens with stiffened sections, it is calculated as the sum of the center-line length of the tubes and the nominal center-line length of the inner stiffeners. The former part is calculated using the same simplified method as the specimens with unstiffened sections while the latter length equals to the sum of the widths of all inner stiffeners. The yield strengths of unformed steel plates (f_{yv}) are estimated from the measured yield strengths of the planar coupons considering a standard strength enhacement in the cold-formed planar plates. According to previous studies by Hu et al.[16] and Guo et al.[13], a strength enhancement of 9% and 4% were respectively considered for the 6-mm and 10-mm thick plates, respectively. As an alternative, the average measured yield stress $\sigma_{0.2}$ of the planar plates shown in Table 1 is also used as the strength f_{yv} directly to predict the sectional strength, designated as $f_{ya,GB2,}$

for comparison.

5.3 Analysis and comparison

The calculated sectional yield stresses $f_{ya,AISI}$, $f_{ya,GB}$ and the ratios of the calculated strengths to the experimental strength, i.e., $f_{ya,AISI}/f_{u,exp}$, $f_{ya,GB}/f_{u,exp}$, and $f_{ya,GB2}/f_{u,exp}$ are presented in Table 2. Fig. 13 shows the variation of the ratio of the predicted strengths to the experimental strength with the ratio of stiffener area. The results and comparisons are discussed as follows:

(1) The AISI method appears to overestimate the sectional strength for the unstiffened and partially stiffened 6-mm thick columns (SHS-a-6 and SHS-b-6) by more than 10%, but slightly underestimate in the cases of well-stiffened 6-mm columns and all the 10-mm thick columns with the ratio $f_{ya,AISI}/f_{u,exp}$ ranging from 0.92 to 0.99. By relating to the failure modes discussed in Section 3, the above comparison is generally in line with the trend of local buckling, in that when local buckling is still a significant factor such as the cases of SHS-a-6 and SHS-b-6, an over-prediction of the sectional strength occurs; otherwise the method appears to predict reasonably well the sectional strength albeit slightly on the conservative side.

(2) The GB method, on the other hand, appears to predict well for all cases where the stiffening effect was less significant, which included two 6-mm thick columns SHS-a-6 and SHS-b-6 due to none or insufficient stiffeners, and all 10-mm thick columns except SHS-e-10. As discussed in Section 3, due to the large thickness in the SHS-10 series columns the stiffenening enhancement only became somewhat significant in the heavily stiffened case of SHS-e-10 (A_s/A = 0.26). However, the GB method markedly under-predicts the sectional strength in the three well-stiffened 6-mm columns (SHS-c-6, SHS-d-6 and SHS-e-6, with A_s/A ranging from 0.15 to 0.3) by more than 10%, and in SHS-10-e by 7%. This comparison seems to suggest that while the GB method may be considered as generally satisfactory when

extended to SHS columns with thick walls, it tends to become overconservative for well-stiffened cases.

(3) From the comparison calculations for the GB method using the planar plate strength instead of the unformed steel strength as the basic strength, the predicted stress $f_{ya,GB2}$ are generally greater than the test strength $f_{u,exp}$. The mean value and standard deviation (SD) of all the ratios $f_{ya,GB}/f_{u,exp}$ are 1.02 and 0.06, respectively. This indicates that using the GB code method on the basis of the planar plate strength will tend to be generally on the unsafe side for the category of cold-formed SHS columns under consideration.

6. Conclusions

A comprehensive study has been presented concerning the strength capacities of cold-formed SHS columns with thick walls and the effect of stiffeners in such cases. Coupon tests were carried out to investigate the strength enhancement in the corner, weld, and planar parts of the sections due to the cold-forming process, and stub column tests were conducted to evaluate the overall sectional strength. Two typical methods generally adopted in the calculation of the sectional strength of cold formed thin-walled members, namely the AISI and GB methods, were evaluated for their applicability in the cases of the thick-walled members under consideration. Based on the results, the following conclusions may be drawn:

a) The yield strength (proof stress $\sigma_{0.2}$) of the corner and weld regions from the test sections exhibit significant strength enhancement, as expected. Measuring by the increase of strength relative to the planar plates, the enhancement was 23.3% (corner) and 22.3% (weld) in the 6-mm thick plates, and 13.6% (corner) and 32.3% (weld) in the 10-mm thick plates. The planar plates themselves were estimated to have an increase in strength comparing to the corresponding unformed plates by 9% and 4% in the 6-mm and 10-mm thickness cases, respectively. Such level of strength enhancement confirms that this factor should also be appropriately considered in the design of cold-formed sections with thick walls.

b) Generally speaking, the 6-mm SHS columns still exhibited a noticeable level of “thin-walled” features, in that local buckling still tends to govern the ultimate strength. As such, the use of stiffeners was observed to play an effective role in terms of enhancing the local buckling resistance and thus increasing the overall sectional capacity.

c) When the wall thickness increased to 10mm, the ultimate strength still appeared to be associated with wall buclking; however due to the much reduced slendness, the effectiveness of the stiffeners appeared to diminish regardless of the width of the stiffeners. The use of stiffeners only appeared to demonstrate a marked enhancement effect when 8 stiffeners, with two on each side of the section, were applied.

d) With all the above influencing factors, an accurate prediction of the sectional strengths for this category of cold-formed section is understandably complicated. The application of the AISI method tends to show an overestimation of the sectional strength for the unstiffened and partially stiffened 6-mm thick columns by a margin of more than 10%, but only slightly underestimate in the cases of well-stiffened 6-mm columns and all the 10-mm thick columns. In comparison, the GB method appears to predict well for all cases where the stiffening effect was less significant for the groups of columns tested, but underestimates the sectional strength in the well-stiffened 6-mm and 10-mm columns by a margin of more than 10% and about 4%, respectively.

The finite element analysis, though limited in the scope within this paper, was able to reproduce favourably the overall strength and deformation capacities, as well as the damage process and failure modes. This paves a way for extended investigation into the change of the response and failure patterns as the wall thickness and the section dimensions vary in a wider range beyond what is covered in the present study. A more systematic evaluation on the effective use of stiffeners taking into consideration of the column dimensions, as well as the

wall thickness, will also need to be conducted with the aid of computer simulation in conjunction with necessary experiments.

Acknowledgements

The authors gratefully acknowledge the supports of the National Natural Science Foundation of China (No. 51108204), the Science Foundation of Ministry of Education of China (No. 20100142120072) and the Fundamental Research Funds for the Central Universities (No. 2014QN210).

References

[1] Ellobody, B., and Young, B. Behavior of cold-formed steel plain angle columns. Journal of Structural Engineering, 2005(131):457-466.

[2] Silvestre, N., Dinis, P. B., and Camotim, D. Developments on the design of cold-formed steel angles. Journal of Structural Engineering, 2013(139):680-694.

[3] Young, B. Research on cold-formed steel columns. Thin-walled Structures, 2008(46):731-740.

[4] Yap, D. C. Y., and Hancock, G. J. Experimental study of high-strength cold-formed stiffened-web C-sections in compression. Journal of Structural Engineering, 2011(137):162-172.

[5] Nguyen, V. B., Wang, C., Mynors, D. J., English, M. A., and Castellucci, M. A.Compression tests of cold-formed plain and dimpled steel columns. Journal of Constructional Steel Research, 2012, 69 (1): 20-29.

[6] Gardner, L., Saari, L., and Wang, F. Comparative experimental study of hot-rolled and cold-formed rectangular hollow sections. Thin-walled Structures, 2010, 48 (7):495-507.

[7] Afshan, S., Rossi, B., and Gardner, L. Strength enhancements in cold-formed structural sections-Part I: Material testing. Journal of Constructional Steel Research,

2013(83):177-188.

[8] Zhu, J., and Young, B. Cold-formed-steel oval hollow sections under axial compression. Journal of Structural Engineering, 2011(137):719-727

[9] American Iron and Steel Institute (AISI). North American specification for the design of cold-formed steel structural members. AISI, Washington, DC. 2007

[10] Australian/New Zealand Standards (AS/NZS). Cold-formed steel structures. AS/NZS 4600, Sydney, Australia,2005

[11] Chinese Standard (GB).Technical code of cold-formed thin-wall steel structures. GB 50018, National Standard of PRC, Beijing ,China, 2002

[12] Macdonald, M., Heiyantuduwa, M. A., and Rhodes, J.. Recent developments in the design of cold-formed steel members and structures. Thin-walled Structures, 2008, 46(7-9):1047-1053.

[13] Guo, Y., Zhu, A., and Pi Y. Experimental study on compressive strengths of thick-walled cold-formed sections. Journal of Constructional Steel Research, 2007, 63(5):718-23.

[14] Yu, W. Cold-formed steel design (3rd Edition). ISBN 0-471-34809-0, United States of America, 2000

[15] Tao, Z., Wang, Z., and Han, L. Behavior of rectangular cold-formed steel tubular columns filled with concrete. Engineering Mechanics, 2006, 23(3):147-155. (In Chinese).

[16] Hu, S., Ye, B., and Li, L. Materials properties of thick-wall cold-rolled welded tube with a rectangular or square hollow section. Construction and Building Materials, 2011, 25(5): 2683–2689.

[17] Rossi, B., Afshan, S., and Gardner, L. Strength enhancements in cold-formed structural sections-Part II: Predictive models.” Journal of Constructional steel Research, 2013(83): 189-196.

[18] Tong, L., Hou, G., Chen, Y., Zhou, F., Shen, K., and Yang, A. Experimental investigation

on longitudinal residual stresses for cold-formed thick-walled square hollow sections. Journal of Constructional steel Research, 2012(73):105-116.

[19] Tang, Y., and Ye, W. A handbook of testing technique in civil engineering. Tongji University Press, Shanghai, China, 1999

[20] Abdel-Rahman, N., and Sivakumaran, K. S.. Material properties models for analysis of cold-formed steel members. Journal of Structural Engineering, 1997(123): 1135-1143

[21] Jia, L., Tsuyoshi, K., and Hitoshi, K. Experimental and numerical study of postbuckling ductile fracture of heat-treated SHS stub columns. Journal of Structural Engineering, 2014, 140(7): 165-180.

Table 1. Measured specimen dimensions and test results of steel coupons

Specimen	A_0 (mm^2)	σ_u (MPa)	Average σ_u (MPa)	$\sigma_{0.2}$ (MPa)	Average $\sigma_{0.2}$ (MPa)	Δ (%)
P-6-1	215.32	574.70		461.41		
P-6-2	226.17	495.50	537.37	406.91	437.88	
P-6-3	223.05	541.90		445.33		
W-6-1	206.58	622.10		585.87		
W-6-2	214.56	566.10	582.00	525.73	535.54	22.3%
W-6-3	216.58	557.80		495.01		
C-6-1	97.76	562.60		521.69		
C-6-2	96.29	633.50	614.00	529.65	539.76	23.3%
C-6-2	89.80	645.90		567.93		
S-6-1	186.67	516.40		409.81		
S-6-2	188.85	537.20	531.63	411.65	410.79	
S-6-3	184.66	541.30		410.92		
P-10-1	340.87	451.00		424.12		
P-10-2	345.16	442.10	445.67	372.09	381.68	
P-10-3	338.79	443.90		348.83		
W-10-1	352.20	523.10		507.13		
W-10-2	359.35	538.30	526.93	505.50	505.00	32.3%
W-10-3	366.05	519.40		502.36		
C-10-1	333.30	495.10		432.04		
C-10-2	303.23	504.60	495.47	435.31	433.55	13.6%
C-10-3	318.49	486.70		433.30		
S-8-1	244.97	579.60		499.53		
S-8-2	245.51	528.50	551.07	410.04	453.59	
S-8-3	242.43	545.10		451.18		

Table 2. Summary of the test and calculated strengths of the cold-formed SHS columns

Specimens	r_i/t	A (mm^2)	A_s/A	$N_{u,exp}$ (kN)	$\Delta N_{u,exp}$ (%)	$f_{u,exp}$ (MPa)	$\Delta f_{u,exp}$ (%)	$f_{ya,AISI}$ (MPa)	$f_{ya,GB2}$ (MPa)	$N_{u,FEA}/N_{u,exp}$	$f_{ya,AISI}/f_{u,exp}$	$f_{ya,GB}/f_{u,exp}$	$f_{ya,GB2}/f_{u,exp}$
SHS-a-6	1.70	4568.3	0	1830		400.59		454.76	449.95	0.94	1.14	1.03	1.12
SHS-b-6	1.59	5104.0	0.10	2070	13.11	405.57	1.24	450.58	444.88	1.00	1.11	1.01	1.10
SHS-c-6	1.35	5613.7	0.17	2560	35.27	456.03	13.67	447.17	440.97	1.08	0.98	0.89	0.97
SHS-d-6	1.60	6186.6	0.23	2840	39.45	459.05	12.82	443.46	437.33	1.05	0.97	0.87	0.95
SHS-e-6	1.63	6647.7	0.30	3050	42.96	458.81	12.68	441.16	434.86	1.10	0.96	0.87	0.95
SHS-a-10	1.56	7309.4	0	3060		418.64		399.69	443.48	1.00	0.95	1.02	1.06
SHS-b-10	1.48	8020.8	0.08	3370	10.13	420.16	0.36	400.87	435.60	1.07	0.95	1.00	1.04
SHS-c-10	1.30	8631.6	0.15	3570	15.13	413.60	-1.20	400.74	436.04	1.06	0.97	1.01	1.05
SHS-d-10	1.32	9470.4	0.21	3830	21.57	404.42	-3.44	401.07	423.55	1.13	0.99	1.01	1.05
SHS-e-10	1.44	9905.6	0.26	4320	32.90	436.12	4.32	402.87	420.24	1.01	0.92	0.93	0.96
Mean										1.04	0.99	0.97	1.02
SD										0.03	0.07	0.06	0.06

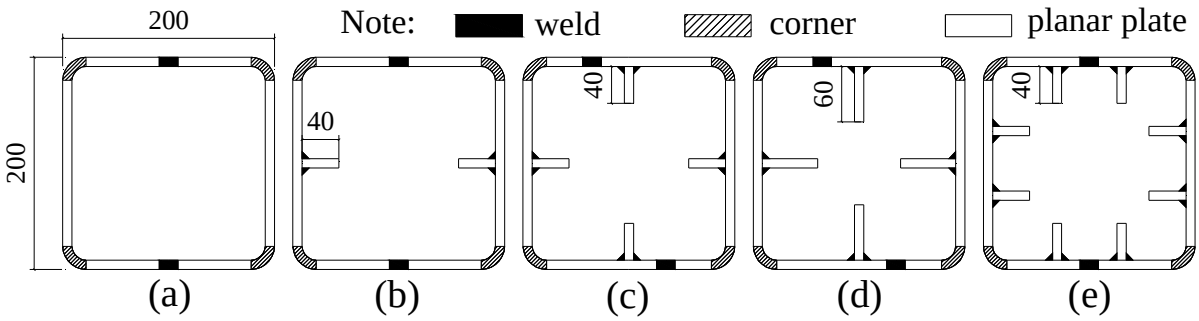

Fig. 1. Unstiffened and stiffened sections considered in this study

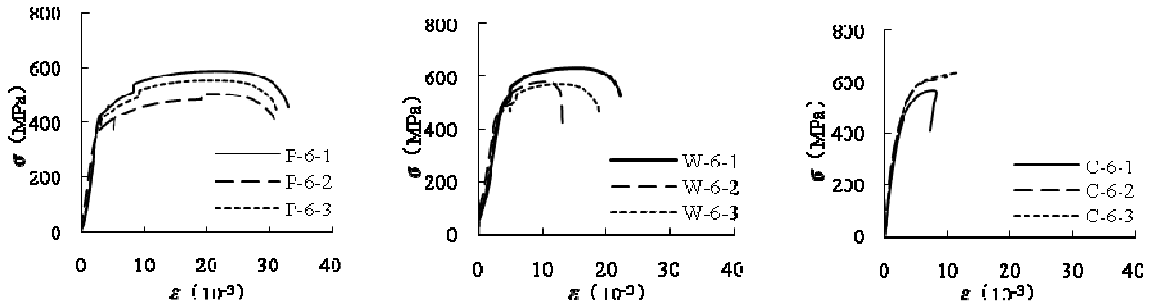

(a) Planar coupons (b) Welded coupons (c) Corner coupons

Fig. 2. σ-ε curves of steel coupons with thickness of 6mm

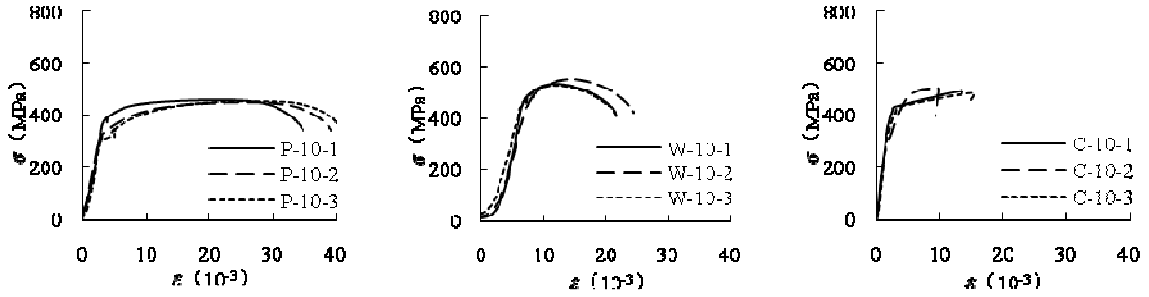

(a) Planar coupons (b) Welded coupons (c) Corner coupons

Fig. 3. σ-ε curves of steel coupons with thickness of 10mm

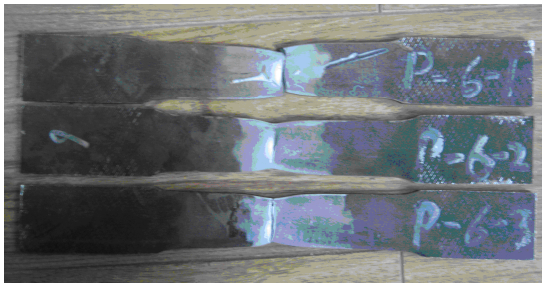

(a) Planar coupons

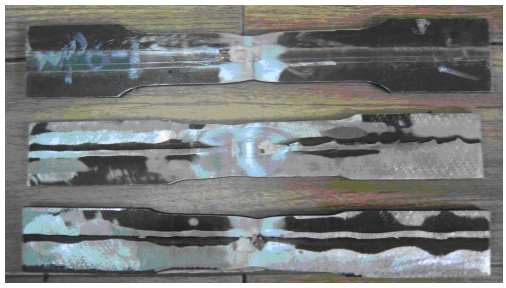

(b) Weld coupons

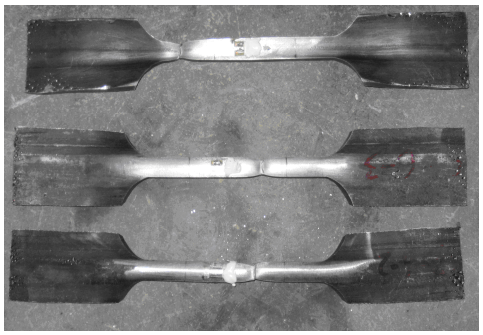

(c) Corner coupons

Fig. 4. Typical failure modes of coupon specimens

Fig. 5. Test setup of cold-formed SHS stub columns

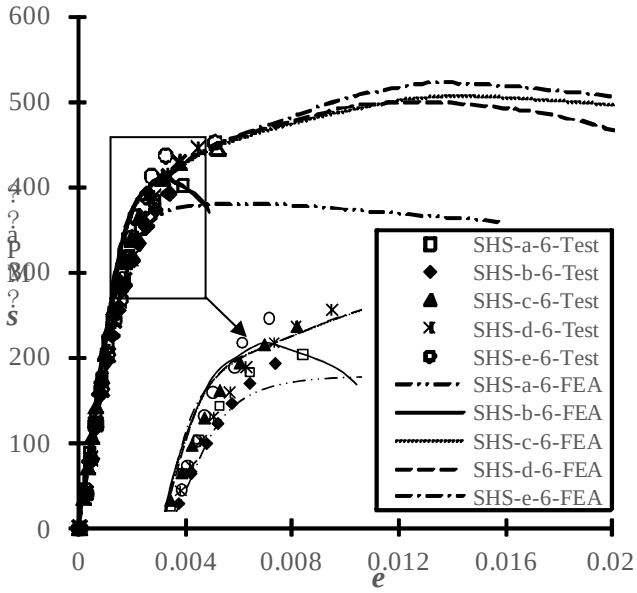

Fig.6. σ-ε curves of 6-mm thick SHS columns

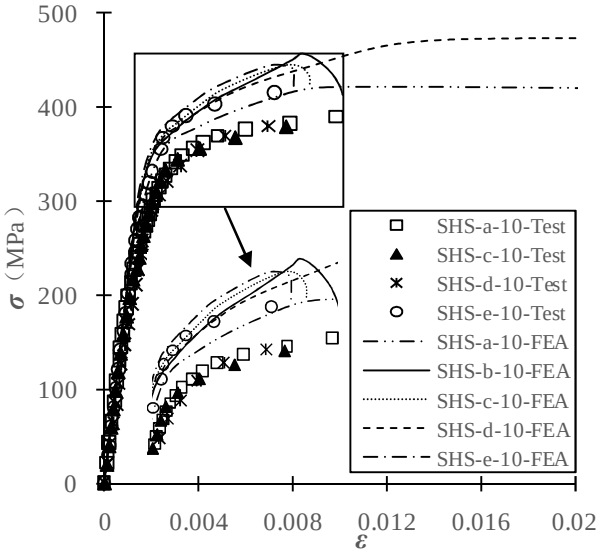

Fig.7. σ-ε curves of 10-mm thick SHS columns

(a) SHS-a-6 (b) SHS-b-6 (c) SHS-c-6 (e) SHS-d-6 (e) SHS-e-6

Fig. 8. Typical failure modes for 6-mm thick SHS columns (circles indicate locations of apparent buckling and will be compared with FE results in Fig. 12)

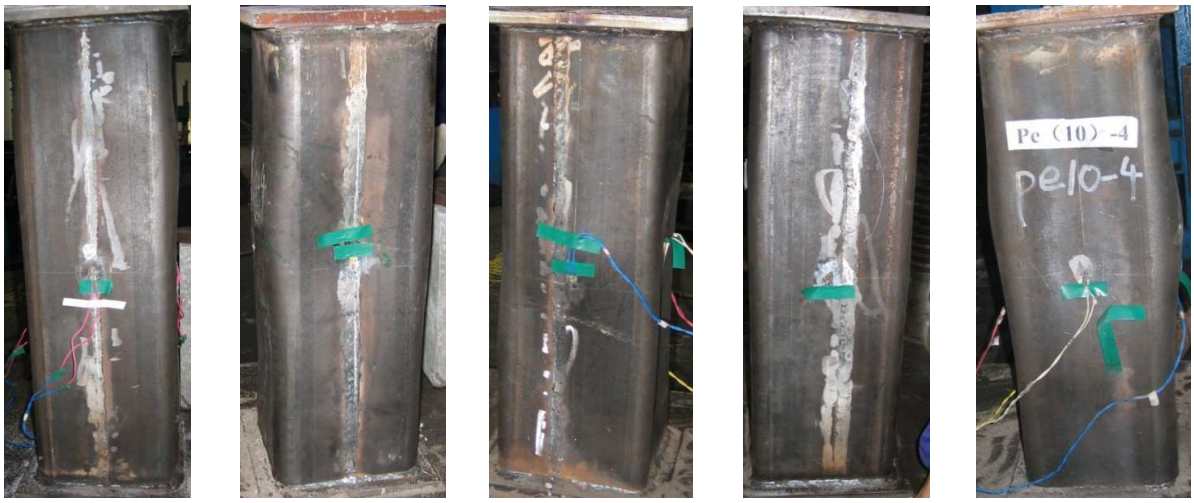

(a) SHS-a-10 (b) SHS-b-10 (c) SHS-c-10 (e) SHS-d-10 (e) SHS-e-10

Fig. 9. Typical failure modes of SHS 10-mm thick SHS columns

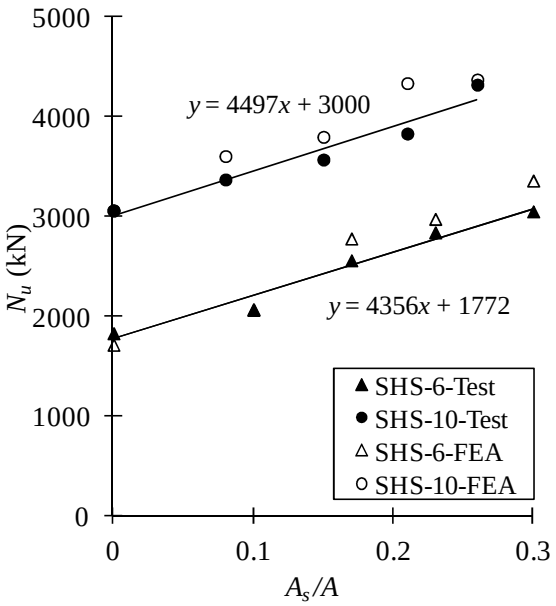

Fig. 10. Variation of $N_{u,exp}$ and $N_{u,FEA}$ with ratio A_s/A

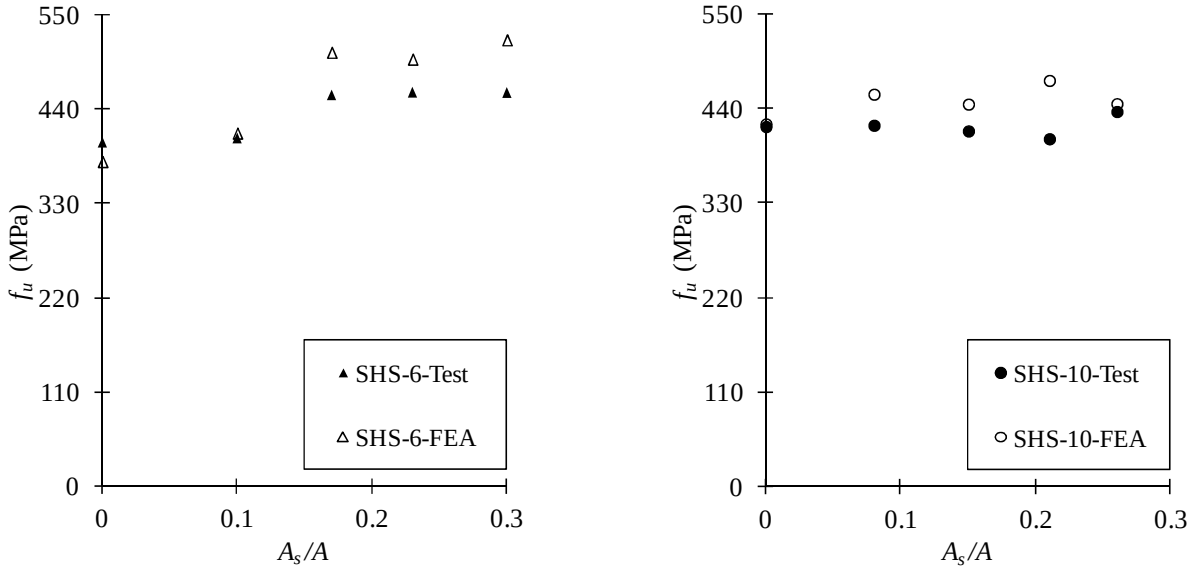

(a) Columns of 6mm thickness (b) Columns of 10mm thickness

Fig. 11. Variation of $f_{u,exp,}$ and $f_{u,FEA}$ with ratio A_s/A

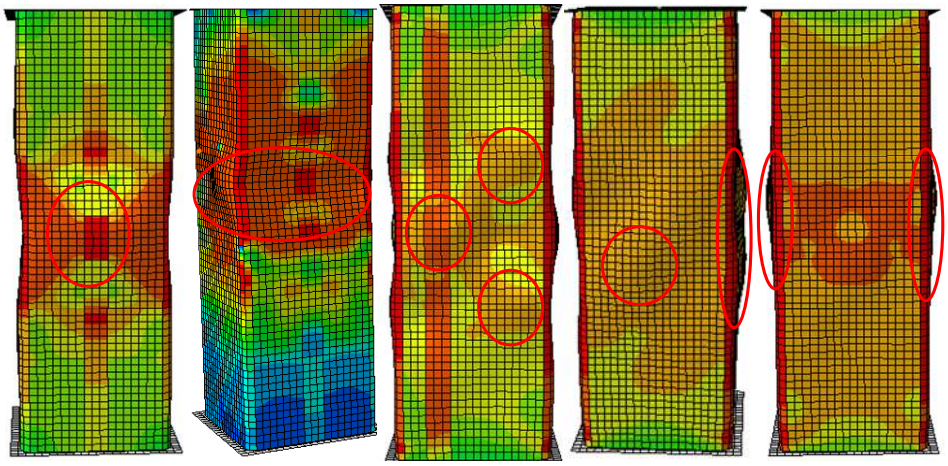

(a) SHS-a-6 (b) SHS-b-6 (c) SHS-c-6 (d) SHS-d-6 (e) SHS-e-6

Fig. 12. Typical failure modes obtained from FE analysis

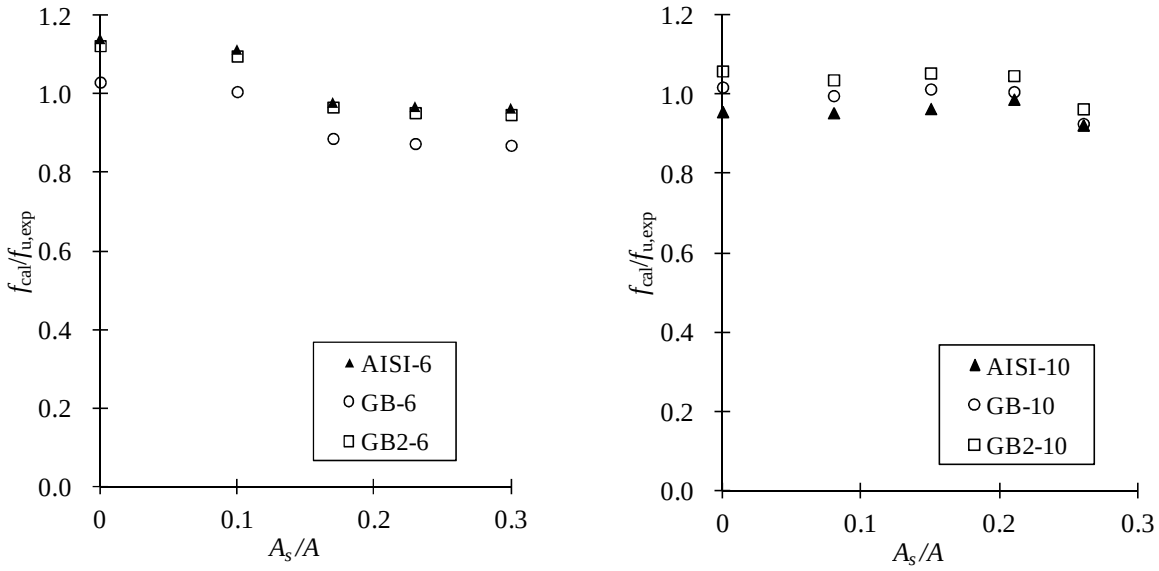

(a) Columns of 6mm thickness (b) Columns of 10mm thickness

Fig. 13. $f_{cal}/f_{u,exp}$ versus A_s/A curves